Water Science and Engineering, 2012, 5(2): 210-218
doi:10.3882/j.issn.1674-2370.2012.02.009

http://www.waterjournal.cn
e-mail: wse2008@vip.163.com

Safety evaluation of replacement reinforcement quality in abutment contact zones of ultra-high arch dam in first impoundment period based on prototype monitoring

Bo HU[1, 2], Zhong-ru WU[2], Guan-biao LIU[1], Bin ZHAO[1], Bo XU*[2]

1. NARI Group Corporation, State Grid Electric Power Research Institute, Nanjing 210003, P. R. China
2. College of Water Conservancy and Hydropower Engineering, Hohai University, Nanjing 210098, P. R. China

Abstract: Reinforcement quality evaluation at the abutment is an important research direction. Prototype monitoring and theoretical derivation were integrated to study the replacement reinforcement quality in abutment contact zones of the Xiaowan ultra-high arch dam. The principles of monitoring layout and design are introduced in detail. Prototype monitoring shows that the increment of the interfacial compressive stress is much larger in the impoundment stage than in the regulating stage. The water pressure and time-effect are two main factors affecting the interfacial stress. The time-effect is the key factor in the initial impoundment stage, and the water pressure is the key factor after impoundment. The contact properties are significantly improved by grouting. This study shows that there are three typical stages in the joint opening hydrographs, namely the compression stage, opening stage, and stable stage. There is a nonlinear relationship between the joint opening and temperature, which can be well described by the S-function. In conclusion, the reinforcement effect is satisfying, and the abutment is safe.

Key words: *ultra-high arch dam; prototype monitoring; compressive stress; joint opening; safety evaluation*

1 Introduction

The abutment is one of the key parts of an ultra-high arch dam. Replacement reinforcement is usually used to enhance the rock mass quality at the abutment. The contact zone mechanical property between rock masses and replacement bodies has a direct impact on the load-transfer performance of the arch thrust. The interface mechanical property will directly affect the safety of projects and economic benefit. It is an important research direction in engineering mechanics, with high scientific value and practical significance (Wu et al. 2011; Duan et al. 2011; Jin et al. 2011).

This work was supported by the National Natural Science Foundation of China (Grant No. 51139001), the Natural Science Foundation of Jiangsu Province (Grant No. BK2009479), the Scientific Research Foundation of the State Human Resource Ministry for Returned Chinese Scholars (Grant No. 2009003), the Scientific Research Foundation for Doctors in Jiangsu Enterprises (Grant No. 2011-33), and the Jiangsu Provincial Postdoctoral Sustentation Fund (Grant No. 1101049C).
*Corresponding author (e-mail: *xubo0214@163.com*)
Received Feb. 28, 2011; accepted Feb. 27, 2012

Prototype monitoring is one of the most intuitive and reliable research methods (Wu 2003). Because of the complexity of the interface mechanics and geological conditions, it is difficult to apply the theoretical results directly to practical projects. There are some difficulties in theoretical analysis, such as simplifying the model and determining boundary conditions. There are also some difficulties in laboratory tests of rock mechanics and reduced-scale model tests, such as representative sampling, comparability between the analysis model and prototype model, and the size effect of rock masses. The numerical analysis is also not a panacea, with problems including the selection of calculation parameters and definition of discontinuities (Hu and Liu 2011; Su et al. 2011). Based on the data from prototype monitoring, the mechanical response of the dam and rock masses can be captured. It is helpful to the understanding of the project operation state and safety factors.

In order to enhance the strength of surrounding rock masses at the right abutment of the Xiaowan Dam, some weak rock masses were excavated and replaced with concrete. The quality of replacement reinforcement was evaluated based on prototype monitoring in this study. The mechanical behaviors in contact zones between the replacement bodies and the rock masses were discussed and analyzed. The distribution and evolution of interfacial compressive stresses and joint openings in contact zones are discussed in detail. The prototype monitoring and theoretical derivation were integrated in this study.

2 Project overview

2.1 Engineering situation

The Xiaowan Dam, with a height of 294.5 m, is being constructed on the Lancang River in Yunnan Province in Southwest China, and is mainly for power generation. The project also has the functions of shipping, irrigation, flood control, tourism, and other comprehensive functions. It is currently under construction. After completion of the project, there will be a reservoir with a storage capacity of 14.9 km^3. The total generating capacity of the project will reach 4 200 MW.

The valley is deep and V-shaped. The hydrogeological conditions are very complicated. The main lithology is granitic gneiss. The highest unloading relaxation depth reaches 160 m. This is mainly due to the complicated geological conditions and processes, such as fluvial erosion. The rock quality at the abutment is very low. Integrated approaches including replacement, high-pressure consolidation grouting, and pre-stressed anchoring, were used to improve the rock quality at the abutment. Thick slurries under high pressures were used in grouting, and the grouting pressure reached 5 MPa. The original water-cement ratio was 1:1. Integrated methods, including the rock mass water pressure test, wave velocity test, static elastic modulus test, and core boring test (Hu et al. 2011; Wu et al. 2009), were used to inspect the grouting effect.

2.2 Principles of monitoring design

Ten-layer replacement holes (about 1 745 m) were designed for the force-resisting bodies

at the right abutment according to the following principles (Zhao et al. 2008):

(1) The monitoring items and monitoring layout should be set to analyze the reinforcement quality. The design should meet the requirements.

(2) According to the monitoring requirements, various monitoring items should be set to prove one another. An overall plan should be made, and all factors should be taken into consideration. Furthermore, the weak areas of the project should be emphasized.

(3) To obtain correct information, the monitoring technique should be reliable, practical, and advanced, and the monitoring method should be easy to operate.

(4) The economic rationality should be taken into consideration.

2.3 Monitoring items and layout

The plan view and arch crown cross-section of the Xiaowan Dam are shown in Fig. 1.

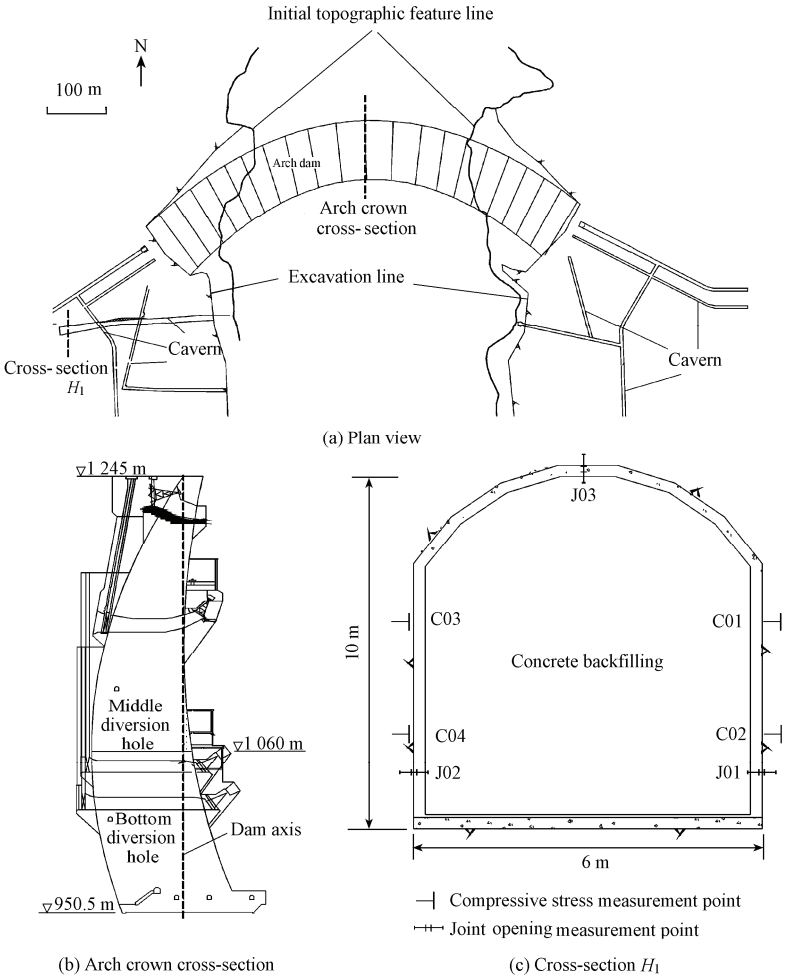

Fig. 1 Structure diagram and monitoring layout

There are two main items in monitoring design: the interfacial compressive stress and joint opening, which were measured with the compressive stress meter and joint opening

meter. The measurement ranges of the two instruments are 0 to 6.0 MPa and 0 to 25 mm, respectively, and the accuracies are ±1.0% and ±0.1%, respectively. The compressive stress meter consists of 140 sensors, while the joint opening meter consists of 179 sensors. Taking section H_1 as an example, the typical monitoring layout is shown in Fig. 1(c). C01, C02, C03, and C04 are the measurement points of the compressive stress, and J01, J02, and J03 are the measurement points of the joint opening.

2.4 Typical operating conditions

There are three stages in the first impoundment period: the first impoundment stage, regulating stage, and second impoundment stage, classified by four typical operating conditions. The storage hydrograph is shown in Fig. 2. The first impoundment stage, regulating stage, and second impoundment stage experience about 20 d (from June 30 to July 20), 20 d (from July 20 to August 10), and 10 d (from August 10 to August 20), respectively.

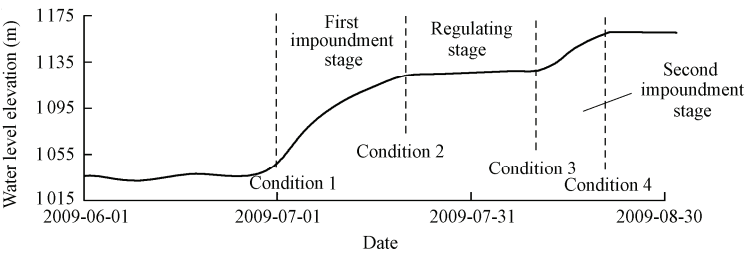

Fig. 2 Storage hydrograph

3 Results and discussion

3.1 Interfacial compressive stress

3.1.1 Stress distribution

As mentioned above, 140 sensors were installed in contact zones between rock masses and backfill concrete, normal to the loading direction, to measure the interfacial stress σ. The measured values were divided into four categories: Class A (σ <–2 MPa), Class B (–2 MPa ≤ σ <– 0.5 MPa), Class C (– 0.5 MPa ≤ σ <0 MPa), and Class D (no compressive stress detected).

The distributions of the interfacial stress under different impoundment conditions are shown in Table 1. The proportions of the compressive stress within three ranges (σ <0 MPa, Class A, and Class C) increased with the water level. The rising rate of the compressive stress in the impoundment stages is higher than that in the regulating stage. The proportion of Class C is the highest, and that of Class A is the lowest in the four categories. Under Condition 4, more than 80% of the interfaces were compacted and the compressive stress was not too high (with a magnitude lower than 2 MPa). The results show that the replacement bodies and rock masses are in good contact, that the hydraulic thrust load can be easily transferred to the force-resisting

bodies on banks, and that the compressive stresses in contact zones are much lower than the compressive strength, which is beneficial to the safety of the project.

Table 1 Proportions of interfacial stress in different impoundment conditions

Impoundment condition	Proportion of interfacial stress (%)		
	σ < 0 MPa	Class A	Class C
1	67.1	1.4	35.7
2	80.0	3.6	42.1
3	81.4	3.6	43.6
4	86.4	5.7	44.3

3.1.2 Typical hydrographs

Information about the interfacial stresses at the measurement points C01 and C03 in three stages is provided in Table 2 and Fig. 3.

Table 2 Interfacial stress increment in different stages

Measurement point	Impoundment stage	Stress increment (MPa)	Stress increment per water head (MPa·m^{-1})	Stress increment per day (MPa·d^{-1})
C01	First impoundment stage	–0.283 1	–0.003 5	–0.014 2
	Regulating stage	–0.033 1	–0.010 3	–0.001 7
	Second impoundment stage	–0.490 7	–0.015 8	–0.049 1
C03	First impoundment stage	–0.132 4	–0.001 6	–0.006 6
	Regulating stage	–0.017 5	–0.005 4	–0.000 9
	Second impoundment stage	–0.145 2	–0.004 7	–0.014 5

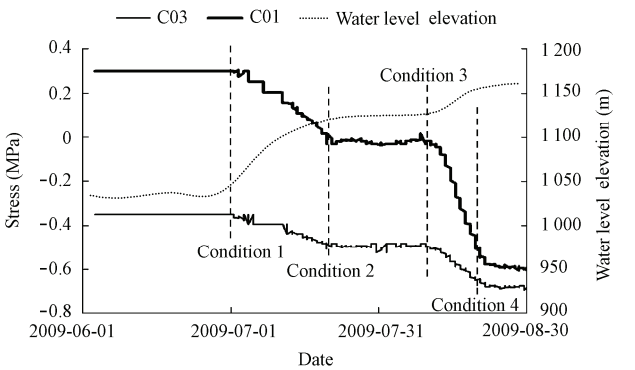

Fig. 3 Typical hydrographs of interfacial stress

Fig. 3 shows a good correlation between the interfacial stress and impoundment process. The compressive stress increment in the impoundment stage is much higher than that in the regulating stage, and the increment at high water levels in the second impoundment stage is higher than that at low water levels in the first impoundment stage.

During the impoundment process, part of the water load was transferred gradually to the force-resisting bodies under the arch-beam effect, leading to an increase of the interfacial compressive stress during the process. This study shows that the arch-effect is more

significant at the high water level, when a higher proportion of the water load is shared by the force-resisting bodies on banks. Thus, the interfacial compressive stress increment per water head in the second impoundment stage is much higher than that in the first impoundment stage.

3.1.3 Model analysis

We selected the water pressure, atmospheric temperature, and time-effect as the main impact factors. Because the temperature changed little during the analysis period from June 1, 2009 to August 30, 2009, the numerical model of the interfacial stress can be described as follows:

$$\hat{\sigma}(t) = \hat{\sigma}_{\mathrm{H}}(t) + \hat{\sigma}_{\theta}(t) \tag{1}$$

$$\hat{\sigma}_{\mathrm{H}}(t) = a_0 + \sum_{i=1}^{n} a_i H^i \tag{2}$$

$$\hat{\sigma}_{\theta}(t) = c_0 + \sum_{i=1}^{p} c_i I_i \tag{3}$$

where $\hat{\sigma}(t)$, $\hat{\sigma}_{\mathrm{H}}(t)$, and $\hat{\sigma}_{\theta}(t)$ are the fitted values of the interfacial stress, the water pressure component, and the time-effect component, respectively; t is time; a_0, a_i, c_0, and c_i are undetermined coefficients; H is the reservoir water level; I_i (i = 1, 2, 3, and 4) is the time function in different forms, where $I_1 = t$, $I_2 = \ln(t+1)$, $I_3 = t^{0.5}$, and $I_4 = \mathrm{e}^{-t}$; n = 4; and p = 4. The analysis results are shown in Table 3 and Fig. 4.

Table 3 Measured and calculated results of interfacial stress

Measurement point	Operation condition	Stress (MPa)		Proportion of different components (%)		Statistical parameter	
		Measurement	Calculation	Water pressure	Time-effect	*R*	*S*
C01	1	0.300 1	0.303 3	3.2	96.8	0.999	0.010
	2	0.017 0	0.011 1	94.9	5.1		
	3	–0.016 1	–0.024 9	91.6	8.4		
	4	–0.506 8	–0.519 9	95.4	4.6		
C03	1	–0.349 3	–0.352 3	2.6	97.4	0.996	0.010
	2	–0.481 7	–0.481 5	94.3	5.7		
	3	–0.499 2	–0.498 7	95.7	4.3		
	4	–0.644 4	–0.657 4	98.4	1.6		

Note: *R* is the multiple correlation coefficient, and *S* is the surplus standard deviation.

The fitting effect is satisfying, with surplus standard deviations less than 0.02 and multiple correlation coefficients higher than 0.99, showing that the water pressure and the time-effect are the key influencing factors in interfacial stresses. The controlling factor changes in different stages: the time-effect is dominant in the initial impoundment stage, while the water pressure is dominant after impoundment. The time-effect component reaches 95% in Condition 1, while the water pressure component is higher than 90% in conditions 2, 3, and 4.

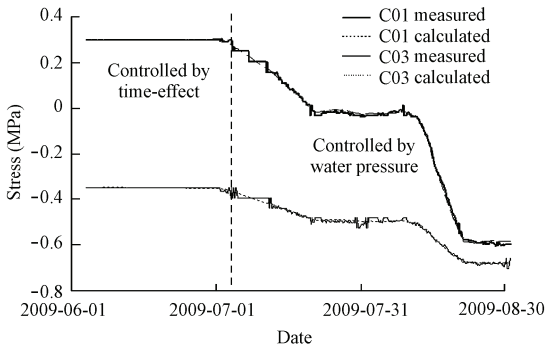

Fig. 4 Comparison of measured and calculated results of interfacial stress

3.2 Joint opening

3.2.1 Effect of grouting

There were some gaps between the replacement bodies and rock masses because of concrete contraction during solidification. In order to enhance the density in contact zones, consolidation grouting was used.

The distribution of different sizes of joint openings is shown in Table 3. The positive values indicate that the joint opening is larger than the reference value, and vice versa. The joint openings declined substantially after grouting, with the mean value of the openings decreasing from 0.92 mm to 0.05 mm, showing a good effect of grouting.

Table 3 Distribution of joint openings

State	Proportion of different sizes (%)				Mean value of opening (mm)
	> 1.0 mm	0-1.0 mm	–0.5-0 mm	< –0.5 mm	
Before grouting	33.3	35.9	28.2	2.6	0.92
After grouting	0	37.4	57.4	5.2	0.05

3.2.2 Typical hydrographs

Typical hydrographs are shown in Fig. 5. There are three typical stages in the joint opening hydrograph, namely the compression stage (*OA*), opening stage (*AB*), and stable stage (*BC*). In the early stage of instrument installation, the temperature in contact zones rises rapidly because of a large amount of hydration heat released. Then the volume of concrete and rock masses expands, and the joints are compacted (*OA*). This does not indicate that the joints are compressive. The measurement results are relative values compared with the initial condition. Thus, to evaluate the conditions of contact zones, other physical quantities (such as the contact compressive stress) should be considered. With the decrease of the temperature during the process of thermal diffusion, the concrete shrinks, and the joint opening increases (*AB*). When the temperature stabilizes, the joint openings tend to be stable, with a little change (*BC*).

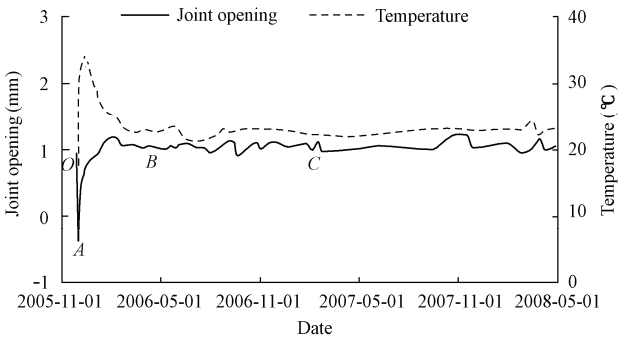

Fig. 5 Hydrographs of joint opening and temperature

3.2.3 Correlation analysis between joint opening and temperature

The linear fitting method, polynomial fitting method, and S-function fitting method were used to study the relationship between the joint opening and temperature. The correlation analysis results in Fig. 6 show that the S-function fitting method is the best method. This is because of the non-linear relationship between the joint opening and temperature.

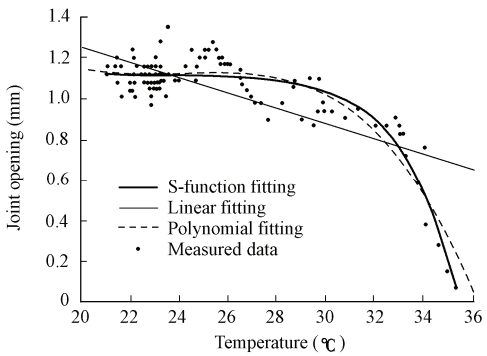

Fig. 6 Regression analysis of joint opening and temperature

4 Conclusions

Prototype monitoring and theoretical derivation were integrated to study the replacement reinforcement quality in abutment contact zones of the Xiaowan ultra-high arch dam. The following conclusions are drawn:

(1) The interfacial compressive stresses increase with the rise of the reservoir water level. The replacement bodies and rock masses are in good contact, and the arch thrust can be well transferred to the force-resisting bodies on banks. The compressive stresses in contact zones are much lower than the compressive strength, which is beneficial to the safety of the project.

(2) This research shows a good correlation between interfacial compressive stresses and the impoundment process. The increment of the interfacial compressive stress is much higher in the impoundment stages than in the regulating stage, and the increment at high water levels in the second impoundment stage is higher than that at low water levels in the first impoundment stage.

(3) Water pressure and the time-effect are the key factors in interfacial compressive stresses. The controlling factor changes in different stages: the time-effect is dominant in the initial impoundment stage, while the water pressure is dominant after impoundment.

(4) The grouting has a good effect. The joint openings decline substantially after grouting, with a mean value of joint openings decreasing from 0.92 mm to 0.05 mm.

(5) There are three typical stages in the joint opening hydrographs, namely the compression stage, opening stage, and stable stage. There is a non-linear relationship between the joint opening and temperature, which can be well described by the S-function.

In conclusion, the weak geological bodies are well replaced, and the abutment is safe.

Acknowledgements

The authors would like to thank Hong PENG, Zhi-yuan WANG, Lin PAN, Shi-dong HAN, Hui SHEN, Xiao-li GOU, and Jun-sheng CHEN for their support of this research.

References

Duan, S. H., Ren, Q. W., Chen, J. P., and Li, Q. 2011. Study on the performance of arch dam influenced by relaxation of the foundations following excavation. *Science China (Technological Sciences)*, 54(5), 1177-1182. [doi:10.1007/s11431-011-4345-9].

Hu, B., and Liu, G. B. 2011. Evaluation and research on replacement reinforcement quality at abutment of ultra-high arch dam based on prototype monitoring. *Proceedings of International Symposium on Modern Technologies and Long-term Behavior of Dams*, 243-251. Beijing: China WaterPower Press.

Hu, X. H., Wu, F. Q., and Sun, Q. 2011. Elastic modulus of a rock mass based on the two parameter negative-exponential (TPNE) distribution of discontinuity spacing and trace length. *Bulletin of Engineering Geology and the Environment*, 70(2), 255-263. [doi:10.1007/s10064-010-0321-z].

Jin, F., Hu, W., Pan, J. W., Yang, J., Wang, J. T., and Zhang, C. H. 2011. Comparative study procedure for the safety evaluation of high arch dams. *Computers and Geotechnics*, 38(3), 306-317. [doi:10.1016/j.compgeo.2010.10.008]

Su, H. Z., Wen, Z. P., and Wu, Z. R. 2011. Study on an intelligent inference engine in early-warning system of dam health. *Water Resources Management*, 25(6), 1545-1563. [doi:10.1007/s11269-010-9760-3].

Wu, F. Q., Liu, T., Liu, J. Y., and Tang, X. L. 2009. Excavation unloading destruction phenomena in rock dam foundations. *Bulletin of Engineering Geology and the Environment*, 68(2), 257-262. [doi:10.1007/s10064-009-0202-5].

Wu, Z. R. 2003. *Safety Monitoring Theory and Its Application to Hydraulic Structures*. Beijing: Higher Education Press. (in Chinese)

Wu, Z. R., Peng, Y., Li, Z. C., Li, B., Yu, H., and Zheng, S. R. 2011. Commentary of research situation and innovation frontier in hydro-structure engineering science. *Science China (Technological Sciences)*, 54(4), 767-780. [doi:10.1007/s11431-011-4336-x]

Zhao, B., Zhao, Z. Y., Qiu, X. D., Liao, Z. Y., and Cui, G. 2008. General design of safety monitoring automation system for Xiaowan hydropower station. *Hydropower Automation and Dam Monitoring*, 32(6), 53-57. (in Chinese)

(Edited by Ye SHI)